

Influence of Density of State with Defect in Cu(In,Ga)Se₂ Investigated by Photoluminescence

Woei-Tyng Lin¹, Fang-I Lai¹, Yu-Kuang Liao², Dan-Hua Hsieh³, Hao-Chung Kuo³, and Shou-Yi Kuo^{4,*}

¹ Department of Photonics Engineering, Yuan-Ze University, 135 Yuan-Tung Road, Chung-Li 320, Taiwan, R.O.C.

² Department of Electrophysics, National Chiao Tung University, 1001 Ta Hsueh Road, Hsinchu 300, Taiwan, R.O.C.

³ Department of Photonic & Institute of Electro-Optical Engineering, National Chiao Tung University, 1001 Ta Hsueh Road, Hsinchu 300, Taiwan, R.O.C.

⁴ Department of Electronic Engineering, Chang Gung University, 259 Wen-Hwa 1st Road, Kwei-Shan Tao-Yuan 333, Taiwan, R.O.C.

* Phone: +8863-2118800, ext. 3351, E-mail : sykuo@mail.cgu.edu.tw

1. Introduction

The Cu(In,Ga)Se₂ (CIGS) thin films and its related materials were the promising absorber materials with the fabrication of solar cell has attracted immense research interest because of the wide gap property of $E_g > 1.3$ eV ($x = \text{Ga}/(\text{In}+\text{Ga}) > 0.5$), large absorption coefficient with more than 10^5 cm^{-1} near the band gap region and cheap large-scale deposition of polycrystalline CIGS [1-2]. However, the structural defects have profound effects on performance of CIGS. Photoluminescence (PL) is promising technique for analysis of the crystal quality, impurity, alloy composition and intrinsic recombination in semiconductor. The photoluminescence (PL) of CIGS-based solar cells has recently been studied and the PL spectra have been analyzed by common recombination processes of the donor-to-acceptor pair and band-to-band transitions. In this paper, we further studied the photoluminescence of the CIGS absorber layer to obtain the clear picture of the carrier recombination and lifetime as well as the defect distribution and efficiency in the CIGS by using temperature-depended, excitation-depended photoluminescence with different performance.

2. Experiment

The Cu(In,Ga)Se₂ absorption layer was prepared on a Mo coated Soda-lime glass (SLG) by three stage coevaporation method. The average alloy composition with $[\text{Cu}]/([\text{In}]+[\text{Ga}])$ and $[\text{Ga}]/([\text{In}]+[\text{Ga}])$ (GGI) ratio was around 0.65 and 0.25-0.30 respectively. The as-deposited CIGS thin film had been further fabricated into a CIGS solar cell with structure of ZnO:Al (AZO)/ZnO/CdS/CIGS/Mo/SLG with the efficiency of 10-12%. These samples of Cu(In,Ga)Se₂ absorption layer were measured by photoluminescence which were carried out by diode laser working at wavelength of 635nm with continuous wave mode and power equal to 1-50 mW as an excitation source. The performance of CIGS solar cells were measured by J-V measurement at an irradiation intensity of 1000 W/m^2 , AM1.5G, and room temperature.

3. Results and discussions

PL spectrum was measured under the excitation power of 50mW with temperature about 10K shown in Fig. 1. There were three and four peaks appearing at CIGS _{$\eta=10\%$} (black opened square) and CIGS _{$\eta=12\%$} (red opened circle) respectively. As PL spectra, the given 3 peaks of CIGS _{$\eta=10\%$} were $p_1=0.929$ eV, $p_2=0.998$ eV, $p_3=1.085$ eV, and 4 peaks of CIGS _{$\eta=12\%$} were $p_1=0.974$ eV, $p_2=1.054$ eV, $p_3=1.138$ eV and $p_4=1.190$ eV, respectively. The p_1 and p_2 of CIGS _{$\eta=10\%$} and CIGS _{$\eta=12\%$} are dominated emission process which typically depend on the donor-acceptor pair (DAP) transition in CIGS. According to CIGS films with GGI ratio p_3 of CIGS _{$\eta=10\%$} were represented to free-to-bound recombination with the photo-holes trapped energy by acceptors, and p_3 and p_4 of CIGS _{$\eta=12\%$} were attributed to near-band-edge (NBE) recombination [3] and degenerated electron to valence band recombination in CIGS respectively. The integrated PL intensity reveal CIGS _{$\eta=12\%$} was 1.5 times the internal quantum efficiency of the CIGS _{$\eta=10\%$} , and implied the PL spectrum intensity was associated with the efficiency of CIGS solar cell.

The CIGS samples also used the Temperature dependent PL measurement with temperature range 10-300 K, in which the spectrum of CIGS _{$\eta=10\%$} at 140K appeared the other emission peak at high energy side ~ 1.172 eV which respected to the near-band-edge recombination of CIGS _{$\eta=10\%$} . The thermal activation energy E_a , E_b of the CIGS films can be obtained using the PL intensity from 10 to 300 K, and is found to be $E_{a(\eta=10\%)} = 23$ meV, $E_{b(\eta=10\%)} = 6$ meV and $E_{a(\eta=12\%)} = 92$ meV, $E_{b(\eta=12\%)} = 8$ meV, respectively. Mechanisms for thermal quenching of the PL signals in CIGS films include localized effects and relaxed by nonradiative recombination process, which E_a was correlated to Gaussian distribution of fluctuations of potential, and E_b was related to the thermal release of carriers trapped at nonradiative centres. The inhomogeneous composition of metal atoms or complicated alloy influence the potential energy and cause the localization about 6-8 meV on the carrier dynamics. However, $E_{b(\eta=12\%)}$ was a factor of 4 that for $E_{b(\eta=10\%)}$ implied that the defects or nonradiative centers of CIGS _{$\eta=10\%$} were likely to be present more than of CIGS _{$\eta=12\%$} .

The power-dependend PL spectrum with variation of excitation power (I_{exc}) from 1 mW to 50 mW at 10K was measured as Fig. 2 (a). To deserve to be mentioned, the CIGS films had the “competition” phenomenon between the DA1 (p1) and DA2 (p2) recombination. It happens a similar case in the the power-dependend PL spectrum of $CIGS_{\eta=12\%}$. The results reveal a fact of the A2 acceptor with larger concentration than that of A1 acceptor in $CIGS_{\eta=10\%}$. Therefore, the intensity of p2 started to decrease and that of p3 was increased while the excitation power above 40 mW, where it revealed that the donor state was filled by excited electrons and more electrons tend to occupy the conduction band then to recombination with A2 acceptor. To compare with the ratio of intensity p2 over p1 (I_{p2}/I_{p1}) between $CIGS_{\eta=10\%}$ and $CIGS_{\eta=12\%}$ shown as Fig. 2 (b), the DA2 transition of $CIGS_{\eta=12\%}$ began grabbing the donors bring about the DA1 recombination rate decreased after $I_{exc} = 5$ mW, that occurred later than the the DA2 transition of $CIGS_{\eta=10\%}$. Moreover, the slope of I_{p1}/I_{p2} for $CIGS_{\eta=10\%}$ was larger than for $CIGS_{\eta=12\%}$ obviously with excitation power above 10 mW. These results of intensity of p2 over p1 indicated that the density of A1 state of $CIGS_{\eta=12\%}$ was more than of $CIGS_{\eta=10\%}$, and the density of A2 $CIGS_{\eta=10\%}$ of state was much more than of $CIGS_{\eta=12\%}$.

The characterization of the solar cell and the corresponding J-V curves were shown in Fig. 3. The open-circuit voltage of the devices increases with the increased bandgap in the CIGS films. The short-circuit current was increased substantially about 17.4%. We conjecture that this behavior insinuated to the short-circuit current increased for $CIGS_{\eta=12\%}$ not only be influenced by the decreased bandgap in CIGS films but also by the quantity of nonradiative centers in CIGS films. The results can be described by a standard diode model with an ideal p-n junction cell equation:

$$J(V) = J_0 \exp\left(\frac{q(V-R_s I)}{AKT}\right) - J_0 - J_{sc} + \frac{V-JR_s}{R_p} \quad (1)$$

In eq. (1), R_p is caused mainly by short circuit pathways [4]. The existence of nonradiative centers such as defects caused the photogenerated carrier recombination before be collected by the contact. The diminished nonradiative centers in $CIGS_{\eta=12\%}$ films increased in R_p and reduced the trapping for photogenerated carriers by nonradiative centers during the diffusion to the contacts of the external circuit. The room-temperature J-V analysis carried out the characterization of CIGS solar cell behavior and identified the cause of the performance which has a good agreement with the PL results of CIGS films.

3. Conclusions

We demonstrated the carrier transport dynamics and defect characteristic in CIGS films with the efficiency found to be 10 % and 12 %. The kind and density state of defects were significant influence on performance of CIGS films as well as manifested to luminescence. According to the J-V analysis, the enhanced short-circuit current in

$CIGS_{\eta=12\%}$ was caused by the reduction in nonradiative centers.

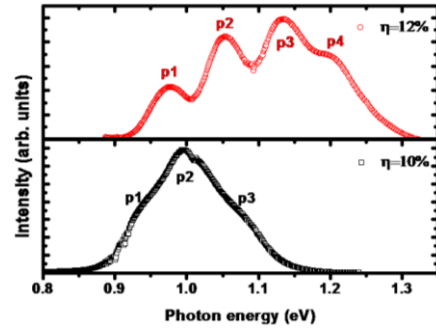


Fig. 1 The PL spectra of the CIGS thin film at 10 K.

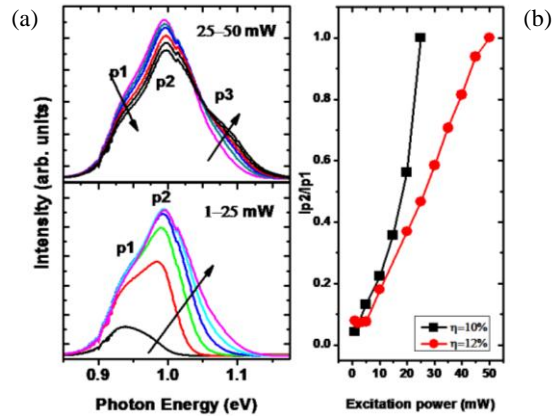


Fig. 2 The PL spectra of the $CIGS_{\eta=10\%}$ under excitation powers from 1 mW to 50 mW.

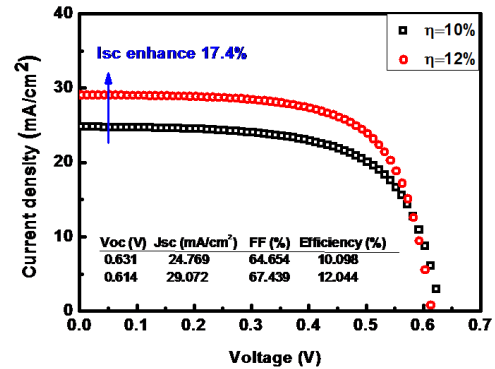


Fig. 3 The J-V curves and parameters of CIGS solar cells

Acknowledgements

The authors would like to thank Compound Semiconductor Solar Cell Department, Next Generation solar cell Division, Green Energy and Environment Research Laboratories, Industrial Technology Research Institute of Taiwan for technical supports.

References

- [1] S. Siebentritt and U. Rau (Eds.), *Wide-Gap Chalcopyrites*: Chap. 6 Springer, Berlin, (2005).
- [2] Kenji Yoshino, Tetsuo Ikari, Sho Shirakata, Hideto Miyake and Kazumasa Hiramatsu, *Appl. Phys. Lett.* 78, 6 (2001).
- [3] W. N. Shafarman and L. Stolt, *Cu(InGa)Se₂ Solar Cells*. In *Handbook of Photovoltaic Science and Engineering*, A. Luque, S. Hegedus (eds). Wiley Sons: Chichester, pp. 567–616 (2003).
- [4] Ya-Ju Lee, Min-Hung Lee, Chun-Mao Cheng, and Chia-Hao Yang, *Appl. Phys. Lett.* 98, 263504 (2011).